J. Phys. Chem. A **2008,** *112,* 8585–8592

Formation of an Ion-Pair Molecule with a Single $NH^+\cdots Cl^-$ Hydrogen Bond: Raman Spectra of 1,1,3,3-Tetramethylguanidinium Chloride in the Solid State, in Solution, and in the Vapor Phase

Rolf W. Berg,*[,†] Anders Riisager,[†,‡] and Rasmus Fehrmann[†,‡]

Department of Chemistry, and Center for Sustainable and Green Chemistry, Technical University of Denmark, Kemitorvet, Building 207, DK-2800 Lyngby, Denmark

Received: April 24, 2008; Revised Manuscript Received: June 4, 2008

Some ionic compounds (salts) form liquids when heated to temperatures in the range of 200−300 °C. They may be referred to as moderate temperature ionic liquids. An example of such a compound is the 1,1,3,3-tetramethylguanidinium chloride, [TMGH]Cl, melting at ∼212 °C. The chemistry of this compound—containing a dimeric ion-pair "molecule"—was investigated in the solid state, in solutions in water and ethanol, and in the vapor phase, based on ab initio molecular orbital density functional theory (DFT)-type calculations with 6-311+G(d,p) basis sets. Calculations on the monomeric $[TMGH]^+$ ion and the dimeric chloride ion-pair salt converged to give geometries near the established crystal structure of [TMGH]Cl. The structures and their binding energies are given as well as calculated vibrational harmonic normal modes (IR and Raman band wavenumbers and intensities). Experimentally obtained Raman scattering spectra are presented and assigned, by comparing to the quantum mechanical calculations. It is concluded that dimeric molecular ion pairs with four $N-H^+\cdots Cl^-$ hydrogen bonds probably exist in the solutions and are responsible for the relatively high solubility of the "salt" in ethanol. It was discovered that the compound can be easily sublimed by heating to about 200−230 °C. In the Raman spectrum of the vapor at 225 °C, a characteristic strong band at 2229 cm^{-1} was found and interpreted to show that the gas phase consists of monomeric ion-pair "molecules" held together by a single $N-H^+\cdots Cl^-$ hydrogen bond, the stretching band of which is causing the band.

Introduction

Ionic compounds being molten at or near room temperature have gained in importance in recent years because of their many interesting properties and potential applications as, e.g., solvents for separation processes.[1] Since the discovery that certain ionic compounds could be vaporized and even distilled at moderate temperatures up to a few hundred degrees Celsius,[2] the properties of the gases have been intensively studied, see, e.g., refs 3−7. Thus, Armstrong et al.[4] have by mass spectrometry found that eight common imidazolium-based ionic liquids evaporate as ionic pairs. Photoelectron spectroscopy on the vapor over 1-ethyl-3-methylimidazolium bis(trifluoromethylsulfonyl)imide have provided similar results.[5] Leal et al.[6] have found by ion cyclotron resonance mass spectrometry that aprotic ionic liquids A^+X^- form a gas phase composed by discrete anion−cation pairs [AX], with no free ions or higher aggregates. However, for the gas phase above the 1-methyl-imidazolium acetate, a protic ionic liquid, the vapor was found to consist of isolated neutral molecules of 1-methyl-imidazole and acetic acid.[6]

We have chosen in this work to study ionic compounds containing the 1,1,3,3-tetramethylguanidinium cation, i.e., $(C_5H_{14}N_3)^+$ or $[((CH_3)_2N)_2C{=}NH_2]^+$ or $[TMGH]^+$. Many of the compounds are liquid at temperatures not too high above room temperature. These compounds are of considerable interest, because of their potential use as effective extraction media for SO_2 and CO_2 recovery from stack gases.[8,9] The chloride compound, [TMGH]Cl, is an example of such a compound, because it readily absorbs SO_2 forming a room-temperature ionic liquid. In order to understand the reasons for the apparent affinity for the compound to absorb the gases, we started this detailed study of the [TMGH]Cl compound, even though it alone is not molten at room temperature.

[TMGH]Cl crystals have previously been isolated[10] and have had their crystal structure solved by single-crystal X-ray diffraction methods.[11] The crystals were found to contain discrete centrosymmetric dimers linked by four classical $N-H^+\cdots Cl^-$ hydrogen bonds. The Raman scattering and most of the IR absorption spectra of the compound were, however, not shown, so we decided to use vibrational spectroscopy as a possible way to study the chemical properties. We also based our study on ab initio molecular orbital calculations that allowed determination of converged $[TMGH]^+$ ion geometries with reasonable bonding systems and allowing assignments of the observed vibrational band transitions in the spectra. Harmonic vibrational frequencies and intensities were calculated to give reasonable fits to the observed spectra (no imaginary vibrational frequencies). Such comparison of experimental structures and spectra with model calculations has been reviewed in detail[12] but was never done for any $[TMGH]^+$ compound.

Experimental Methods and Computational Details

Materials. 1,1,3,3-Tetramethylguanidine (TMG, 99%), hydrochloric acid (37%), ethanol (99%), and diethylether (99%) were all purchased from Aldrich and used as received. (*Caution: Use safety goggles when working with TMG because of eye damage risks*[10]). The 1,1,3,3-tetramethylguanidinium chloride salt, [TMGH]Cl, was prepared by direct neutralization of an

---

* Corresponding author. E-mail: rwb@kemi.dtu.dk. Tel.: +45 45 25 24 12. Fax: +45 45 88 31 36.

[†] Department of Chemistry.

[‡] Center for Sustainable and Green Chemistry.

10.1021/jp803597j CCC: $40.75

ethanolic TMG solution with an equivalent amount of hydrochloric acid by a modification of the previously reported method involving mixing and recrystallization.[10] In a typical procedure, 18 mL of 2.0 M HCl (36 mmol) was cautiously added to a stirred solution of 4.15 g of TMG (36 mmol) in 50 mL of ethanol while maintaining the solution at room temperature (*Caution: The neutralization is highly exothermic*). After continuous stirring for 4 h, the solvent was removed under reduced pressure (50 °C, 1 mbar), leaving the product behind in quantitative yield. The raw product was recrystallized from ethanol/diethylether (1:3), followed by drying under vacuum (50 °C, 0.1 mbar) to produce white crystal needles (yield = 4.92 g, 90%). Found by chemical analysis (%): C, 39.7; H, 9.2; N, 27.3; Cl, 23.2. Calcd for $C_5H_{14}N_3Cl$ (%): C, 39.60; H, 9.31; N, 27.71; Cl, 23.38. Found $T_m = 208-209$ °C. Literature reported: 211−212 °C.[10]

NMR spectra in DMSO-d_6 (25 °C) were recorded on a Bruker AM360 NMR spectrometer to identify the compound, giving peak positions relative to the solvent ($\delta H = 2.50$ ppm, $\delta C = 40.45$ ppm): ^1H NMR (300 MHz, DMSO-d_6) $\delta = 2.29$ (s, 12H; CH_3), 5.59 ppm (s, 2H; NH_2); ^{13}C NMR (75.5 MHz, DMSO-d_6) $\delta = 39.60$ ($N-CH_3$), 161.45 ppm ($N=C$).

Raman Spectroscopy. The samples were studied in small capped or sealed cylindrical tubes. Visible laser light (green 514.5 and 532 nm with nominal power up to 2 W) or near-infrared light (1064 nm with power up to 100 mW) were used to excite Raman spectra of the samples, directly through the glass. Dispersive DILOR-XY and Bruker-IFS66 FRA-106 Fourier transform Raman spectrometers were used as described elsewhere.[13−15] The scattered light was filtered to remove the laser line and collected with liquid N_2 cooled CCD or Ge diode detectors to give unpolarized spectra with spectral resolutions of approximately 2−4 cm^{-1}. For the Fourier transform (FT) instrument more than 400 scans were collected in a range from 3500 (Stokes) to −1000 cm^{-1} (anti-Stokes), at approximately 25 °C. The resulting spectra were averaged and not corrected for the small (estimated <10%) changes in instrument response. The dispersive Raman spectra were repeatedly collected in several overlaid sections that were combined after removal of cosmic spikes. In a few cases where a broad fluorescent background was observed, a seventh-order polynomial was fitted to the background and subtracted, allowing for the essential spectrum to be shown more clearly. The spectra did not depend much on the kind of excitation line. The wavelength scales were calibrated with use of cyclohexane spectra to a precision of about 1 cm^{-1} (dispersive)[16] or better than that (FT).

Infrared Absorption. FT-IR spectra were obtained at approximately 25 °C from pressed disks of polycrystalline powder in KBr (1 mg in 100 mg), measured against similar empty references on a Perkin-Elmer 1710 FT instrument (100 scans). The IR spectral resolution was ~4 cm^{-1}.

Ab Initio Molecular Orbital (MO) Quantum Chemical Calculations. The calculations were performed with the Gaussian 03W[17] program on a Pentium R4 3 GHz personal computer operated under Windows XP. The total geometric/conformational energies of the guessed molecular species were minimized by use of Hartree−Fock/Kohn−Sham density functional theory (DFT) procedures at a level of approximation limited by use of restricted-spin Becke's three-parameter hybrid exchange functional (B3), Lee−Yang−Parr correlation and exchange functionals (LYP), and with Pople's polarization split valence Gaussian basis set functions, augmented with d- and p-type polarization functions and diffuse orbitals on non-hydrogen orbitals (B3LYP, 6-311+G(d,p)). This level of modeling has proved to be satisfactory to describe, e.g., methanol clusters.[18] The Gaussian 03W software was used as implemented with the modified GDIIS algorithm and with tight optimization convergence criteria.[17] The molecules and ions were taken to be in assumed gaseous free state and without any preassumed symmetry. The vibrational frequencies and eigenvectors for each normal mode were calculated without adjusting the force constants. The results are reproduced in the tables, according to dominating group frequency motions.

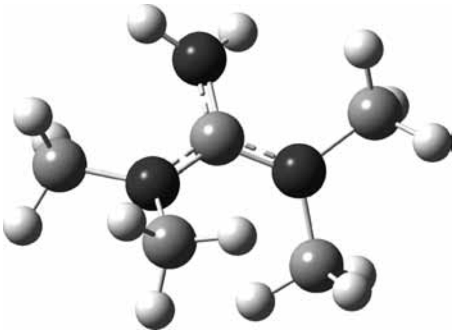

Figure 1. Optimized geometry of the $[TMGH]^+$ ion.

Results and Discussion

$[TMGH]^+$ Ion. For purposes of comparison and to make sure that the Gaussian 03W program[17] performed reasonably well, the structure was optimized and the vibrational spectra of the $[TMGH]^+$ ion calculated. Previous X-ray structural results[11] were reproduced quite closely, as shown in Figure 1 and Table 1 (compare the $[TMGH]^+$ ion column with the experimental data for the $[TMGH]^+$ ion in its chloride salt). It can be seen that the deviations are small, proving—as expected—that reliable structure calculation is possible; the $[TMGH]^+$ ion can be modeled reasonably accurately at the DFT B3LYP/6-311+G(d,p) level.

The calculated numerical spectral values of the isolated $[TMGH]^+$ ion are given in Table 2, together with assignments of calculated bands to normal modes (no imaginary vibrational frequencies). The calculated spectra are reproduced in Figure 2. Experimental spectra of the ion in the [TMGH]Cl salt are given in Figure 3. As may be seen, the calculated spectra are not in perfect agreement with the experimental spectra; especially in the high-wavenumber end of the spectrum and in the IR. The ratio between an experimental wavenumber and a calculated value is commonly referred to as a scaling factor. In many contemporary ab initio quantum chemical calculations near-unit scaling factors (often ca. 0.96−0.97) have been applied to get better agreement between calculated spectra and experimentally found ones. Generally, the need for scaling is due to the deficiencies in the applied models (insufficient modeling of correlation energy, use of inferior basis sets, perturbation from counterions, etc.). Experimental inaccuracies might of course add to the deviations, but the majority hereof should be due to model insufficiency. With respect to the IR, presence of moisture in the KBr matrix and other complications such as crystallite size and refractive index[19] are causing lack of good correspondence between experiment and model. In Raman the situation was better, but still some intensities were too weak and some too strong.

To get a better fit between the model and the experiment, we considered making the experimental conditions closer to that of the model or elaborating on the model.

As a first attempt to come experimentally closer to the isolated $[TMGH]^+$ ion, we tried to examine solutions of the [TMGH]Cl

TABLE 1: Ab Initio Optimized Geometric Structures as Determined by Gaussian 03W DFT B3LYP/6-311+G(d,p) Calculations for an Isolated Tetramethylguanidinium Ion, $[TMGH]^+$, an Isolated [TMGH]Cl Ion Pair, and a Dimeric $[TMGH]_2Cl_2$ Ion Pair, Compared to the Experimental Data in the Crystalline Phase[a,b]

geometric quantity, distance/angle	$[TMGH]^+$ ion	$[TMGH]^+Cl^-$ ion pair	$[TMGH]_2Cl_2$ dimer ion pair	exptl data for $[TMGH]_2Cl_2$ in crystal[a]
N1−C1 (Å)	1.34753	1.32303	1.31688	1.3304(15)
N2−C1 (Å)	1.34400	1.35252	1.36080	1.3417(15)
N3−C1 (Å)	1.34400	1.36578	1.36080	1.3370(14)
C−H (Å)	1.09(1)	1.09(1)	1.09(1)	0.98(1)
N1−C1−N3 (deg)	119.13084	119.38553	120.71332	120.91(10)
N1−C1−N2 (deg)	119.13084	121.67489	120.71348	119.70(10)
N3−C1−N2 (deg)	121.73833	118.93881	118.57320	119.36(10)
C4−N3−C1−N1 (deg)	−21.44330	−20.76242	−19.52591	−23.93(16)
C5−N3−C1−N1 (deg)	146.76858	142.64948	140.86988	151.32(11)
C2−N2−C1−N1 (deg)	−21.44328	−19.00835	−19.52587	−21.74(16)
C3−N2−C1−N1 (deg)	−146.76875	141.13846	140.86759	145.76(11)
N1−H1*A* (Å)	1.00735	1.09913	1.03743	0.918(17)
N1−H1*B* (Å)	1.00735		1.03743	0.886(17)
H1*A*−Cl (Å)		1.83168	2.12989	2.415(17)
H1*B*−Cl (Å)			2.12987	2.373(17)
N1−H1*A*···Cl (Å)		2.91984	3.15944	3.2863(17)
N1−H1*B*···Cl (Å)			3.15942	3.2268(17)
N1−H1*A*−Cl (deg)		169.75346	171.38566	158.4(13)
N1−H1*B*−Cl (deg)			171.38284	168.9(14)
energy	−363.10735630	−823.55982014	−1647.17130188	

[a] Ref 11. [b] The minimum energy calculated is given in atomic units (au, hartree).

salt; it can be dissolved in, e.g., water and in ethanol. The salt solubility in water and ethanol at approximately 25 °C was determined to be around 1.41 and 0.38 g/mL solution, respectively. We recorded the Raman spectra of these solutions, see Figures 4 and 5.

In Figure 4 the experimental Raman spectrum of a nearly saturated aqueous solution is shown. It very much looks like that of the solid plus the water, so the interactions among the $[TMGH]^+$ ions and the Cl^- ions look to be much like in the solid compound and thus not much disturbed by the dissolution process (the presence of the water). Similarly the spectrum of the solvent water is not much influenced by the presence of the solute. An analogous solution spectrum was obtained by Bonner,[20] who, however, did not recognize the origin of the water stretching bands. He also studied the tetramethylguanidinium perchlorate salt (an ionic liquid above 44.5 °C). By osmometry Bonner found $[TMGH][ClO_4]$ in concentrated aqueous solution to form strongly associated ion pairs with two strong $N-H^+\cdots O^-$ hydrogen bonds.[20] This aqueous solution was even claimed to be a nonelectrolyte for more concentrated aqueous solutions. We hence assume that also [TMGH]Cl dimer ion-pair molecules—like those known from the crystal structure—exist in the aqueous solution. Such associations in solution have been found in other solvents[20,21] and may be verified by conductivity, osmotic, or cryoscopy measurements.[22,23]

For [TMGH]Cl dissolved in ethanol (in Figure 5), the experimental CH stretching bands are difficultly discerned on top of the strong bands from CH stretchings of the ethanol (bands near 3000 cm^{-1}). However, bands from [TMGH]Cl are identified at 2820, 1322, 729, 554, 384, and 294 cm^{-1} (indicated by arrows), most markedly the one at 729 cm^{-1}. The *intensities* of the bands of the dissolved salt differ considerably from those of the solid state, indicating that some interaction between the solute and the solvent probably takes place, but we expect that the dimer ion-pair molecules known from the crystal structure will still exist, accounting for the solubility. Salts that do not have the ability to form hydrogen bonds (e.g., of the $N-H^+\cdots Cl^-$ kind) normally have low solubility in ethanol. Also, when comparing Figure 5 to the calculated Raman spectrum for the isolated single $[TMGH]^+$ ion in Figure 2, the accordance between experiment and model is not good. We therefore believe that the solubility of the compound in ethanol is due to the retainment of molecule-like dimeric ion pairs (with four $N-H^+\cdots Cl^-$ hydrogen bonds). Associations in ethanolic solutions have been found in other cases and may be verified by conductivity, osmotic, or cryoscopy measurements.

$[TMGH]_2Cl_2$ Dimer Ion-Pair Molecule Modeling. Next we performed ab initio calculations on a $[TMGH]^+\cdots Cl^-$: $Cl^-\cdots[TMGH]^+$ dimer ion-pair "molecule", aiming at getting a better fit to the experiments. After extended calculation time, the optimized structure shown in Figure 6 was determined. The results of this geometric optimization are included in Table 1, ready for comparison to the experimental geometry data mentioned earlier.[11] Again the experimental structural results were reproduced quite closely (within expected accuracy), proving that reasonably accurate structure modeling is possible at the DFT B3LYP/6-311+G(d,p) level (compare the two last columns).

The vibrational spectra of the dimer ion-pair molecule were also calculated, as shown in Figure 7. The numerical data are given in Supporting Information Table S1. It is seen that the NH_2 vibrations in the two $[TMGH]^+$ ions are much influenced by the presence of the chloride ions: before bonding to the Cl^- anion, NH_2 symmetric and asymmetric stretchings were observed at 3609.6 and 3731.1 cm^{-1}, whereas strong bands at 3068.5 (IR), 3095.8 (Raman), 3097.8 (Raman), 3118.8 (Raman), and 3193.5 (IR) cm^{-1} were observed after the formation of the dimer ion-pair molecule (compare Table 2 mode nos. 59−60 and Supporting Information Table S1, mode nos. 117−118, 122−123), in much better agreement with the observations, e.g., in Figure 3.

[TMGH]Cl Melt. We were interested in seeing what the Raman spectrum would look like in the melt. By heating the salt in a low platinum crucible, covered with a thin glass plate, trying to record the spectrum of the melt we discovered that this was not possible. The melting point is high (ca. 210 °C), and the compound evaporated (sublimed) in the beam already at 200 °C. The sublimate crystals sitting on the glass plate had a Raman spectrum (at room temperature and 100 °C) typical of solid [TMGH]Cl. We tried to put the salt in sealed evacuated

TABLE 2: Calculated Vibrational Spectra for the [TMGH]$^+$ Ion and Assignments

mode no.	wavenumber shifts (cm^{-1})	IR absorption (km/mol)	Raman activity (Å^4/AMU)	depolarization ratio	description of normal mode (assignment)[a]
1	112.7	1.52	0.20	0.75	skeleton def
2	115.8	0.12	0.27	0.19	CN′ twist
3	160.0	0.52	0.55	0.57	CH$_3$ twist
4	182.2	1.53	0.65	0.75	CH$_3$ twist
5	190.9	0.11	1.85	0.41	CH$_3$ twist
6	212.4	4.36	0.14	0.75	CH$_3$ twist
7	237.4	1.38	0.70	0.75	CH$_3$ twist
8	268.4	1.12	0.33	0.61	CH$_3$ twist
9	282.7	5.24	1.14	0.32	NH$_2$ twist
10	329.0	105.24	0.25	0.75	NH$_2$ wag
11	372.0	0.03	2.98	0.23	sym N′C$_2$ deformation
12	375.1	41.31	0.86	0.75	NH$_2$ wag
13	423.1	78.48	0.22	0.75	NH$_2$ wag
14	504.6	4.46	0.16	0.75	NH$_2$ rock
15	536.4	0.01	2.86	0.17	NH$_2$ twist
16	548.7	1.73	1.82	0.35	CN′$_2$ bend
17	712.3	0.10	0.43	0.75	NH$_2$ rock + asym N′C stretch
18	720.2	2.03	18.37	0.06	skeleton breathing
19	867.3	20.96	3.30	0.75	NH$_2$ rock + asym N′C stretch
20	1052.3	8.58	9.68	0.38	CH$_3$ rock + CN$_3$ sym str
21	1065.8	43.91	1.17	0.75	NH$_2$ rock + CH$_3$ rock + N′C str
22	1079.0	12.80	1.77	0.72	CH$_3$ rock
23	1087.9	11.25	1.57	0.75	NH$_2$ rock + CH$_3$ rock + N′C str
24	1126.6	0.28	1.53	0.74	CH$_3$ def
25	1129.1	0.45	0.86	0.75	CH$_3$ def
26	1160.7	6.18	1.93	0.75	CH$_3$ def
27	1162.0	2.74	0.60	0.53	CH$_3$ def
28	1213.4	13.07	0.16	0.75	NH$_2$ rock + CH$_3$ rock + asym N′C str
29	1248.0	7.65	1.26	0.28	CH$_3$ rock + CN str + sym N′C str
30	1272.2	14.67	0.15	0.75	NH$_2$ rock + CH$_3$ rock + asym N′C str
31	1338.1	15.52	10.02	0.10	CN str + CN′$_2$ bend
32	1454.9	59.06	3.95	0.75	CH$_3$ asym umbrella
33	1457.1	15.12	12.22	0.61	CH$_3$ asym umbrella
34	1460.3	27.05	3.34	0.75	CH$_3$ asym umbrella
35	1473.1	9.99	2.87	0.08	CH$_3$ sym umbrella
36	1488.8	14.00	7.18	0.75	CH$_3$ def
37	1497.5	0.63	1.50	0.71	CH$_3$ def
38	1498.4	0.12	20.39	0.73	CH$_3$ def
39	1501.5	46.64	1.93	0.75	CH$_3$ def
40	1513.1	0.02	33.03	0.68	CH$_3$ def
41	1514.0	6.99	1.23	0.75	CH$_3$ def
42	1521.7	2.53	15.48	0.75	CH$_3$ def
43	1522.7	16.46	3.93	0.40	CH$_3$ def
44	1591.8	82.46	1.48	0.41	NH$_2$ sci + CN str
45	1660.5	532.13	1.02	0.75	CN′$_2$ asym str
46	1675.4	274.79	4.69	0.51	NH$_2$ sci + CN str
47	3042.9	31.43	19.69	0.75	CH$_3$ sym str
48	3043.2	8.62	276.80	0.05	CH$_3$ sym str
49	3059.1	12.19	14.59	0.75	CH$_3$ sym str
50	3061.8	20.61	354.74	0.02	CH$_3$ sym str
51	3124.1	6.09	186.47	0.68	CH$_3$ asym str
52	3124.5	15.89	41.81	0.75	CH$_3$ asym str
53	3128.3	0.85	45.69	0.75	CH$_3$ asym str
54	3128.4	0.66	41.96	0.28	CH$_3$ asym str
55	3165.5	2.99	63.07	0.75	CH$_3$ asym str
56	3165.6	1.86	29.85	0.746	CH$_3$ asym str
57	3183.5	7.07	34.62	0.75	CH$_3$ asym str
58	3183.6	0.21	28.04	0.71	CH$_3$ asym str
59	3609.6	117.02	90.63	0.11	NH$_2$ sym str
60	3731.1	81.26	38.37	0.75	NH$_2$ asym str

[a] N′ = N2 and N3.

ampoules, but no good spectra were obtained from the melts, because of strong fluorescence emission when excited by the laser at 532 nm. The melts also turned *faintly* brownish, probably due to *slight* decomposition in the heat. We did not attempt to record the spectrum by excitation with 1064 nm; the blackbody radiation at such a high temperature is too high for the detector of the FT instrument.

[TMGH]Cl Vapor. The observation of the phenomenon of sublimation led us to record the spectrum of the vapor. It has long been believed that ionic liquids (or low-temperature molten salts) would be involatile and exert no measurable vapor pressures, because they would decompose thermally below the vaporization temperature. In connection with the striking experimental results by Earle et al.,[2] demonstrating

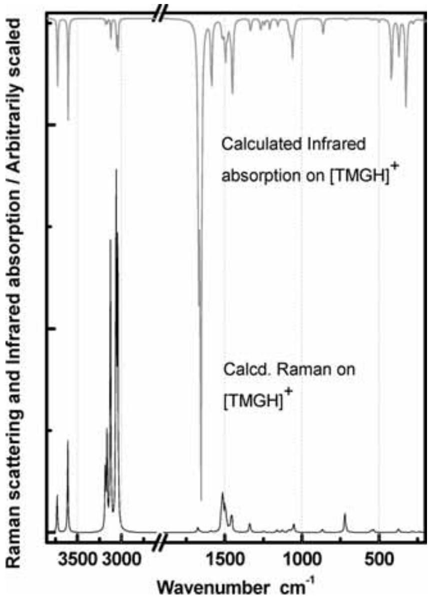

Figure 2. IR absorption (top) and Raman scattering spectra (bottom) of the $[TMGH]^+$ ion calculated in this work by DFT B3LYP/6-311+G(d,p) Gaussian modeling. Curves were arbitrarily scaled and shifted.

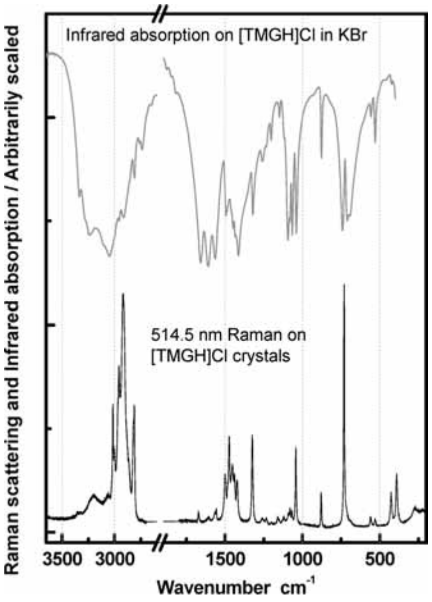

Figure 3. Experimental IR absorption (top) and Raman scattering spectra (bottom) of crystalline [TMGH]Cl obtained in this work. Curves were arbitrarily scaled and shifted.

that many ionic liquids can indeed have a volatility and can be distilled/sublimed, the next question arises: what is the constitution of such vapors? In our case, does the salt [TMGH]Cl vaporize without decomposition forming its gas phase, or does it evaporate/sublime under decomposition/recombination? As a protic ionic compound—in analogy to the 1-methyl-imidazolium acetate studied by Leal et al.[6] that forms a gas phase consisting of isolated neutral molecules 1-methyl-imidazole and acetic acid—the [TMGH]Cl should be expected to form TMG and HCl.

Raman spectra of gases are often very weak.[24] Accordingly, the Raman spectrum of the vapor over the [TMGH]Cl melt at 225 °C (Figure 8) needed to be obtained only after long time excitations at high power. We collected 10 double exposures that were spike filtered and combined (2 h/exposure, 2 W of excitation power). The vapor was contained in 10 mm diameter evacuated and sealed cells, loaded with about 200 mg of [TMGH]Cl and heated to form the vapor in a four-window furnace, designed and built in our laboratory.[14,25] Even the wide diameter was not enough to exclude some signal background from the quartz walls of the cells.

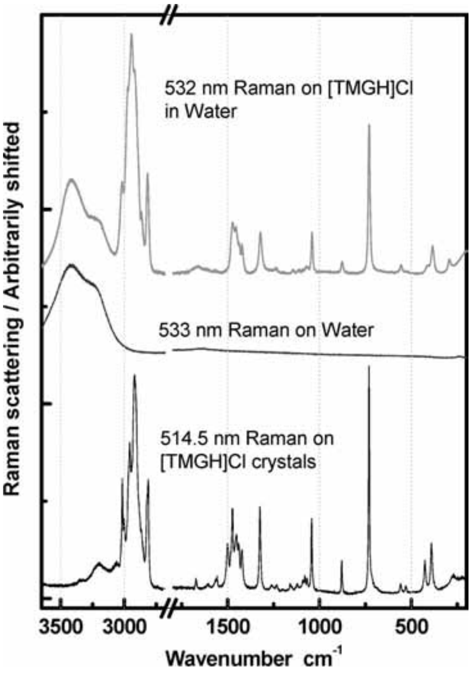

Figure 4. Experimental Raman scattering spectra of crystalline [TMGH]Cl compared to the spectrum of water and a nearly saturated solution in water. Curves were arbitrarily scaled and shifted.

In an attempt to understand and interpret the gas-phase spectra obtained over [TMGH]Cl, we also recorded spectra of TMG vapor and HCl gas (included in Figure 8). The idea of decomposition/recombination would here mean that the following equilibrium reaction is suspected to occur:

$$[\mathrm{TMGH}]\mathrm{Cl(solid)} \rightleftarrows \mathrm{TMG(gas)} + \mathrm{HCl(gas)}$$

The TMG and HCl spectra (in Figure 8) exhibit definite bands, e.g., at 3362 cm^{-1} (N−H stretching, arrow) and 2885 cm^{-1} (H−Cl stretching Q-branch; rotational lines also seen[26,27]).

The DFT B3LYP/6-311+G(d,p) ab initio calculations performed separately on single isolated TMG and HCl molecules resulted in optimized structures with reasonable geometric parameters and minimum energies (−362.70001227 and −460.83282403 au, respectively). N−H stretching and H−Cl stretching frequencies came out at 3525.2 and 2928.2 cm^{-1}, respectively, with predicted strong Raman activities. Clearly we see that the spectrum of the gas phase over [TMGH]Cl does not correspond to this. Hence, we conclude that the gas *cannot* be taken to consist of TMG and HCl molecules. Also, the spectrum of the gas over [TMGH]Cl does not correspond to the spectrum of the $[TMGH]_2Cl_2$ dimer ion-pair molecule; most markedly such a molecule cannot account for the band at 2229 cm^{-1}.

Formation of the Monomeric $[TMGH]^+Cl^-$ Ion Pair. To clarify the situation we performed ab initio calculations on a hypothetical $[TMGH]^+Cl^-$ monomeric ion pair. The determined optimized structure is shown in Figure 9. The results of the geometric optimization are also included in Table 1, allowing for easy comparison with the experimental X-ray crystal structure data for [TMGH]Cl mentioned earlier.[11] As seen, the

TABLE 3: Calculated Vibrational Spectra for the [TMGH]Cl Ion-Pair Molecule and Assignments

mode no.	wavenumber shifts (cm^{-1})	IR absorption (km/mol)	Raman activity ($Å^4$/AMU)	depolarization ratio	description of normal mode (assignment)[a]	Raman observed (cm^{-1})[b,c] (Figure 10)
1	38.52	5.20	0.87	0.74	Cl oopl wag	
2	69.7	8.93	0.55	0.65	Cl ipl rock	
3	112.8	4.80	0.51	0.75	skeleton def	
4	127.0	2.17	0.85	0.50	skeleton def	
5	132.0	6.21	0.95	0.57	skeleton def	
6	157.0	1.80	0.42	0.61	skeleton def	
7	191.0	4.77	1.39	0.21	CH_3 twist	
8	196.9	1.00	1.34	0.75	CH_3 twist	
9	222.0	5.31	0.58	0.75	CH_3 twist	
10	260.5	5.70	0.41	0.75	CH_3 twist	
11	277.8	90.56	2.83	0.11	$Cl\cdots H-N$ str + CH_3 twist	
12	296.6	3.15	0.94	0.75	skeleton def + CH_3 rock	
13	362.2	13.07	1.00	0.26	N_3C rot + CH_3 rock	
14	367.9	3.20	2.37	0.20	$N'C_2$ bend	
15	409.1	17.59	1.45	0.74	$Cl\cdots H-N$ str + CH_3 rock	
16	531.1	30.73	3.67	0.69	NH_2 rock	
17	545.7	2.52	2.20	0.25	CN′2 bend	
18	607.5	72.42	0.87	0.64	NH bend	
19	729.6	8.17	13.97	0.05	skeleton breathing	766 ssp
20	733.0	9.62	8.95	0.18	NH_2 rock + asym N′C stretch	
21	882.6	14.75	3.44	0.75	NH_2 rock + asym N′C stretch	
22	939.2	150.68	20.64	0.75	$Cl\cdots H-N$ oopl bend	812 br
23	1044.7	45.56	11.82	0.36	CH_3 rock	927 wbr
24	1079.0	26.89	0.93	0.74	CH_3 rock	
25	1081.9	14.40	2.99	0.72	CH_3 rock	
26	1116.2	74.98	3.58	0.24	NH_2 rock + CH_3 rock + N′C str	
27	1127.0	3.73	1.34	0.71	NH_2 rock + CH_3 rock + N′C str	
28	1130.9	3.43	0.36	0.69	CH_3 def	
29	1159.4	6.06	0.97	0.65	CH_3 def	
30	1165.5	7.64	2.10	0.66	CH_3 def	
31	1221.0	1.52	1.00	0.72	NH_2 rock + CH_3 rock + asym N′C str	
32	1261.9	15.42	1.01	0.37	CN str + CH_3 rock + asym N′C str	
33	1285.6	14.69	0.57	0.56	NH_2 rock + CH_3 rock	
34	1348.1	3.09	20.31	0.12	sym CN_3 str + CH_3 rock	1049 wbr
35	1440.9	64.80	2.70	0.71	CH_3 umbrella	
36	1450.6	23.46	5.30	0.74	CH_3 umbrella	
37	1453.2	6.93	4.82	0.75	CH_3 umbrella	
38	1462.2	68.85	1.74	0.54	CH_3 umbrella + NH_2 sci	
39	1481.8	7.42	7.98	0.74	CH_3 def	
40	1486.9	17.36	6.15	0.74	CH_3 def	
41	1496.4	3.77	12.86	0.66	CH_3 def + NH_2 sci	1458 mbr
42	1497.2	15.46	5.03	0.75	CH_3 def	
43	1505.4	11.95	8.87	0.75	CH_3 def + NH_2 sci	
44	1509.7	6.21	6.26	0.74	CH_3 def + NH_2 sci	
45	1511.9	4.87	10.41	0.75	CH_3 def + NH_2 rock	
46	1514.8	43.08	4.31	0.61	CH_3 def + NH_2 sci	
47	1572.6	237.31	10.79	0.28	CN str + NH_2 sci + CH_3 def	
48	1603.9	269.24	5.20	0.74	$C-N'_2$ asym str + NH_2 sci + CH_3 def	
49	1652.8	312.38	1.26	0.74	NH_2 sci + CN str	
50	2187.9	3419.7	52.65	0.75	$Cl-H-N$ str	2229 s
51	2997.4	50.11	163.77	0.13	CH_3 sym str	2778 w
52	3017.4	49.24	199.98	0.09	CH_3 sym str	2792 w
53	3024.5	25.73	87.60	0.11	CH_3 sym str	2824 s
54	3030.1	63.02	347.60	0.03	CH_3 sym str	2864 m
55	3064.8	29.60	116.54	0.73	CH_3 asym str	2913 sh
56	3078.3	18.09	88.02	0.74	CH_3 asym str	2957 vs
57	3080.6	13.36	91.98	0.36	CH_3 asym str	2971 msh
58	3099.5	4.07	51.17	0.68	CH_3 asym str	3016 wsh
59	3132.6	4.71	38.69	0.74	CH_3 asym str	
60	3142.1	8.08	41.45	0.72	CH_3 asym str	
61	3150.8	14.76	31.59	0.75	CH_3 asym str	
62	3152.2	0.59	29.74	0.54	CH_3 asym str	
63	3632.9	36.03	86.13	0.19	N−H str	3381 w

[a] N′ = N2 and N3. [b] Abreviations for approximate vibrations: asym = asymmetric, bend = bending, iph = in-phase, ipl = in-plane, ooph = out-of-phase, oopl = out-of-plane, sci = scissoring, str = stretching, sym = symmetric, twist = twisting. Codes for band intensity: m = medium, s = strong, sp = sharp, v = very, w = weak, br = broad. [c] TMG gas was found to have Raman bands at 225 °C at 230 wbr, 304 w, 377 w, 538 w, 564 vw, 737 s, 792 vw, 892 vw, 1071 vw, 1150 vw, 1464 wbr, 1621 m, 2804 s, 2847 s, 2876 s, 2955 vs, 3012 wsh, 3359 s.

calculated structural results gave quite close fits to the parameters of the dimer ion-pair molecule, proving once more that the DFT B3LYP/6-311+G(d,p) modeling is able to predict reasonably accurate structures (compare relevant Table 1 columns). It should be noted that the minimum energy of the ion-pair molecule is −823.55982014 au, i.e., lower than the sum (−823.53283630 au) of the TMG (−362.70001227 au) and HCl (−460.83282403 au) minimum energies from optimizations at

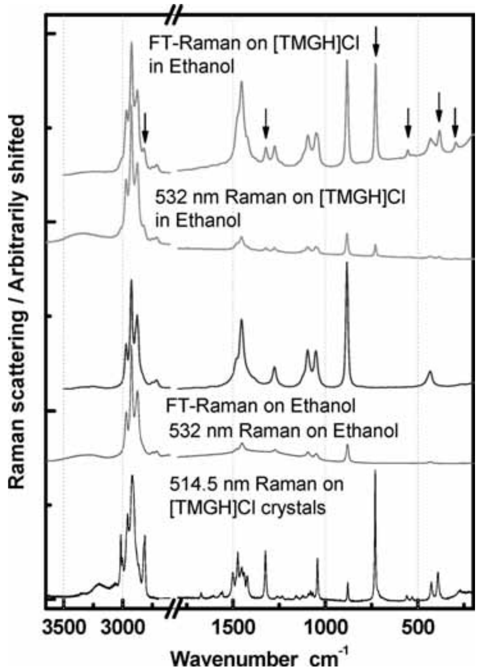

Figure 5. Experimental Raman scattering spectra of crystalline [TMGH]Cl compared to the spectrum of ethanol and a nearly saturated solution in ethanol. The spectra of the solutions were obtained with green and near-infrared excitation without much difference. Curves were arbitrarily scaled and shifted.

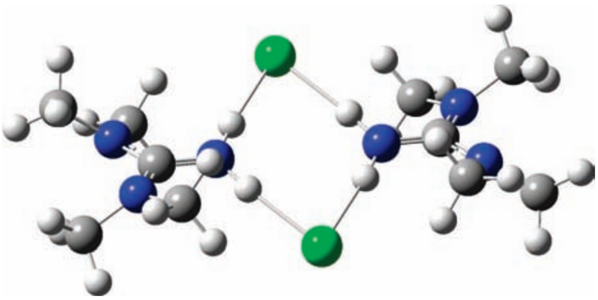

Figure 6. Optimized geometry of the $[TMGH]_2Cl_2$ dimer ion-pair molecule.

similar sophistication levels of modeling, predicting that the ion-pair molecule would be more stable than the separate TMG and HCl molecules.

The calculated Raman spectrum of the ion-pair molecule (no imaginary vibrational frequencies) is compared to the experimental gas-phase spectrum in Figure 10, and the data for the vibrational spectra of the [TMGH]Cl gas molecule are given in Table 3. It is seen that the NH_2 vibrations in the $[TMGH]^+$ ion are much influenced by the bonding to the Cl^- ion. Now we get the NH_2 stretching to split into a NH vibration at ca. 3600 and a $N-H^+\cdots Cl^-$ vibration at ca. 2200 cm^{-1} (compare Table 3). The corresponding experimentally observed bands were found at 3381 (weak) and 2229 (strong) cm^{-1}.

However, it must be admitted that the spectra are not in totally perfect agreement with the spectral observations. But as mentioned before, overestimation of the calculated frequencies should not be taken too seriously, knowing about the approximations involved, knowing about the limitations in the modeling, and being aware of the likely presence of various unaccounted problems like CH_3 Fermi resonance, anharmonicity, etc. Thus all considered, it seems to be quite reasonable to conclude that a [TMGH]Cl monomer ion-pair gas molecule must be present in the gas phase.

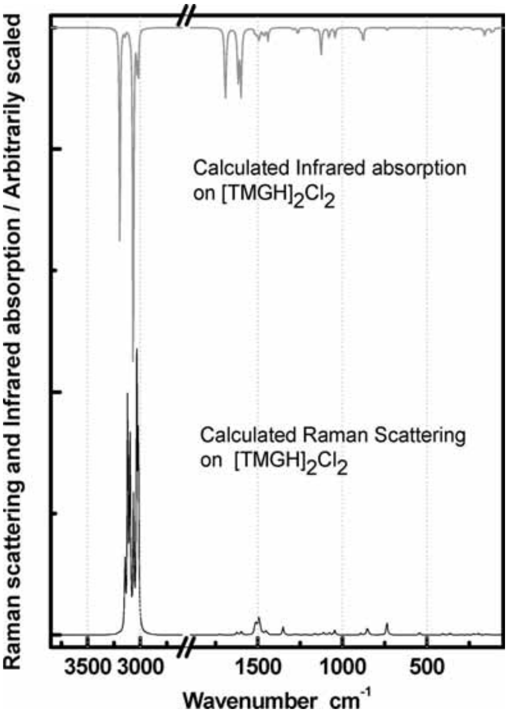

Figure 7. IR absorption (top) and Raman scattering spectra (bottom) of the $[TMGH]_2Cl_2$ dimer ion-pair molecule, calculated in this work by DFT B3LYP/6-311+G(d,p) Gaussian modeling. Curves were arbitrarily scaled and shifted.

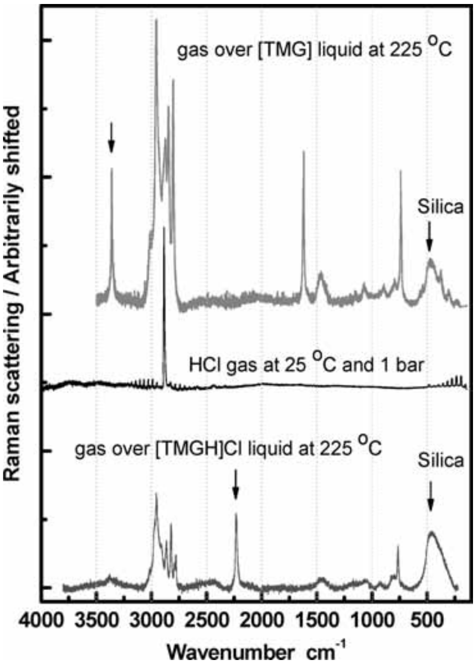

Figure 8. Raman spectra of gases in evacuated and sealed 10 mm diameter ampules at 225 °C over about 200 mg of liquid [TMGH]Cl (bottom) and TMG (top). Also shown (middle) is dry HCl gas at approximately 25 °C and 1 bar. Spectra were obtained by long time exposures (2 h at 2 W of 532 nm excitation power). For position of bands, see Table 3.

Conclusions

The protic compound [TMGH]Cl—in different states—was studied by a combination of Raman spectroscopy and ab initio MO calculations (Gaussian 03W). Convergence to chemically reasonable results was obtained, and the modeling made it possible to grossly understand the observations and determine

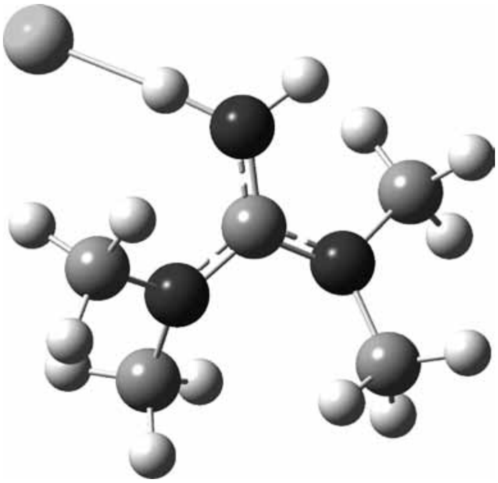

Figure 9. Optimized geometry of the [TMGH]Cl ion pair.

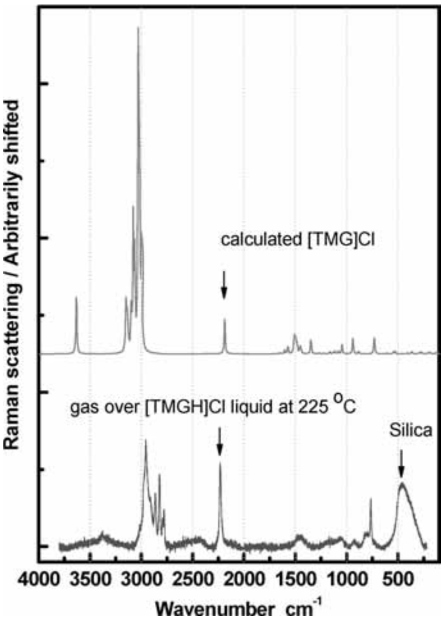

Figure 10. Calculated Raman spectrum of the [TMGH]Cl ion-pair molecule compared to the experimental gas-phase spectrum. The $N-H^+\cdots Cl^-$ hydrogen bond vibration observed at 2229 cm^{-1} is calculated to occur at 2187.9 cm^{-1}, see Table 3.

the most probable species. The compound sublimes/distils above about 200 °C, forming a vapor at 225 °C that most probably consists of monomeric ion-pair molecules held together by one strong $N-H^+\cdots Cl^-$ hydrogen bond that has a characteristic strongly Raman active stretching frequency of about 2229 cm^{-1} (predicted value 2188 cm^{-1}).

Our results here show that the finding by Leal et al.[6] for 1-methyl-imidazolium acetate to split into a vapor of 1-methylimidazole and acetic acid *cannot* be generalized to a universal rule that the gas phase above a protic compound or ionic liquid, $[BH]^+X^-$, should always consist of isolated neutral molecules B and HX. Evidently, Nature seems to be more variable.

Acknowledgment. We thank Professor Irene Shim (DTU, Lyngby, Denmark) for help initiating the computational work. We are grateful to Lykke Ryelund (University of Copenhagen, Denmark) for recording FT Raman spectra. Support from "Lundbeckfonden" (j. no. 177/06) and FTP (j. no. 274-06-0078) are acknowledged, and a Grant from "Direktør Ib Henriksen's Fond" made maintenance of the Raman equipment possible.

Supporting Information Available: Table S1 listing calculated vibrational spectra for the [TMGH]$_2$Cl$_2$ dimer ion-pair molecule, and assignments. This material is available free of charge via the Internet at http://pubs.acs.org.

References and Notes

(1) Berg, R. W. *Monatsh. Chem.* **2007**, *138*, 1045–1075.

(2) Earle, M. J.; Esperança, J. M. S. S.; Gilea, M. A.; Canongia Lopes, J. N.; Rebolo, L. P. N.; Magee, J. W.; Seddon, K. R.; Widegren, J. A. *Nature* **2007**, *439*, 831–834.

(3) Zaitsau, D. H.; Kabo, G. J.; Strechan, A. A.; Paulechka, Y. U.; Tschersich, A.; Verevkin, S. P.; Heintz, A. *J. Phys. Chem. A* **2006**, *110*, 7303–7306.

(4) Armstrong, J. P.; Hurst, C.; Jones, R. G.; Licence, P.; Lovelock, K. R. J.; Satterley, C. J.; Villar-Garcia, I. J. *Phys. Chem. Chem. Phys.* **2007**, *9*, 982–990.

(5) Strasser, D.; Goulay, F.; Kelkar, M. S.; Maginn, E. J.; Leone, S. R. *J. Phys. Chem. A* **2007**, *111*, 3191–3105.

(6) Leal, J. P.; Esperança, J. M. S. S.; Minas da Piedade, M. E.; Canongia Lopes, J. N.; Rebolo, L. P. N.; Seddon, K. R. *J. Phys. Chem. A* **2007**, *111*, 6176–6182.

(7) Akai, N.; Kawai, A.; Shibuya, K. *Chem. Lett.* **2008**, *37* (3), 256–257.

(8) Huang, J.; Riisager, A.; Wasserscheid, P.; Fehrmann, R. *Chem. Commun.* **2006**, 4027–4029.

(9) Huang, J.; Riisager, A.; Berg, R. W.; Fehrmann, R. *J. Mol. Catal. A: Chem.* **2008**, *279*, 170–176.

(10) Anderson, M. L.; Hammer, R. N. *J. Chem. Eng. Data* **1967**, *12*, 442–447.

(11) Fischer, A. K.; Jones, P. G. *Acta Crystallogr.* **2002**, *E58*, o218–o219.

(12) Berg, R. W. *Z. Naturforsch.* **2007**, *62A*, 157–168.

(13) Berg, R. W.; Deetlefs, M.; Seddon, K. R.; Shim, I.; Thompson, J. M. *J. Phys. Chem. B* **2005**, *109*, 19018–19025.

(14) Brooker, M. H.; Berg, R. W.; von Barner, J. H.; Bjerrum, N. J. *Inorg. Chem.* **2000**, *39*, 4725–4730.

(15) Berg, R. W.; Maijó Ferré, I.; Cline Schäffer, S. J. *Vib. Spectrosc.* **2006**, *42*, 346–352.

(16) Berg, R. W.; Nørbygaard, T. *Appl. Spectrosc. Rev.* **2006**, *41*, 165–183.

(17) Frisch, M. J.; Schlegel, H. B.; Scuseria, G. E.; Robb, M. A.; Cheeseman, J. R.; Montgomery, J. A., Jr.; Vreven, T.; Kudin, K. N.; Burant, J. C.; Millam, J. M.; Iyengar, S. S.; Tomasi, J.; Barone, V.; Mennucci, B.; Cossi, M.; Scalmani, G.; Rega, N.; Petersson, G. A.; Nakatsuji, H.; Hada, M.; Ehara, M.; Toyota, K.; Fukuda, R.; Hasegawa, J.; Ishida, M.; Nakajima, T.; Honda, Y.; Kitao, O.; Nakai, H.; Klene, M.; Li, X.; Knox, J. E.; Hratchian, H. P.; Cross, J. B.; Adamo, C.; Jaramillo, J.; Gomperts, R.; Stratmann, R. E.; Yazyev, O.; Austin, A. J.; Cammi, R.; Pomelli, C.; Ochterski, J. W.; Ayala, P. Y.; Morokuma, K.; Voth, G. A.; Salvador, P.; Dannenberg, J. J.; Zakrzewski, V. G.; Dapprich, S.; Daniels, A. D.; Strain, M. C.; Farkas, O.; Malick, D. K.; Rabuck, A. D.; Raghavachari, K.; Foresman, J. B.; Ortiz, J. V.; Cui, Q.; Baboul, A. G.; Clifford, S.; Cioslowski, J.; Stefanov, B. B.; Liu, G.; Liashenko, A.; Piskorz, P.; Komaromi, I.; Martin, R. L.; Fox, D. J.; Keith, T.; Al-Laham, M. A.; Peng, C. Y.; Nanayakkara, A.; Challacombe, M.; Gill, P. M. W.; Johnson, B.; Chen, W.; Wong, M. W.; Gonzalez, C.; Pople, J. A. *Gaussian 03W*, revision B.04; Gaussian, Inc.: Pittsburgh, PA, 2003.

(18) Boyd, S. L.; Boyd, R. J. *J. Chem. Theory Comput.* **2007**, *3*, 54–61.

(19) Berg, R. W. *Spectrochim. Acta* **1975**, *31A*, 1409–1419.

(20) Bonner, O. D. *J. Phys. Chem.* **1979**, *83* (9), 1218–1220.

(21) Hunt, P. A. *J. Phys. Chem. B* **2007**, *111* (18), 4844–4853.

(22) Berg, R. W.; Hjuler, H. Aa.; Bjerrum, N. J. *Inorg. Chem.* **1984**, *23*, 557–565.

(23) Berg, R. W.; Østvold, T. *Acta Chem. Scand., Ser. A* **1986**, *40*, 445–451.

(24) Berg, R. W.; Papatheodorou, G. N. *Inorg. Chim. Acta* **1980**, *45*, L211–L212.

(25) Gilbert, B. P.; Berg, R. W.; Bjerrum, N. J. *Appl. Spectrosc.* **1989**, *43*, 336–341.

(26) Wood, R. W.; Dieke, G. H. *Phys. Rev.* **1930**, *35*, 1355–1359.

(27) Cherlow, J. M.; Hyatt, H. A.; Porto, S. P. S. *J. Chem. Phys.* **1975**, *63* (9), 3996–4000.

JP803597J